CHAPTER VI
n-OCTANE AROMATIZATION ON MONOFUNCTIONAL Pt-Sn/KL CATALYSTS*

6.1 Abstract

The bimetallic Pt-Sn/KL catalysts prepared by different preparation methods, including the various Sn/Pt ratios, have been tested for n-octane aromatization at 500°C and 1 atm. It was found that the addition of tin improved the stability and selectivity to C8-aromatics products, including a decreasing the secondary hydrogenolysis reaction which occurred inside the pores of KL zeolite. The stability of the catalysts and the decrease of the undesired hydrogenolysis reaction were improved by geometric and electronic effects. In addition, Co1Pt1Sn, prepared by vapor phase co-impregnation, yielded a high fraction of alloy phase compared to Seq1Pt1Sn and Seq1Sn1Pt, which were the catalysts prepared by vapor phase sequential impregnation. This PtSn alloy formation causes the electron transfer from tin to Pt atoms as observed from the XPS data. From this electronic effect, OX molecules were more produced as compared to those obtained without the addition of tin. Consequently the EB/OX ratio is lower than unity.

Pt-Sn/SiO$_2$ prepared by incipient wetness co-impregnation yielded a perfect alloy formation and has shown electron transfer from the tin to platinum atoms as observed in Co1Pt1Sn. It was found that Pt-Sn/SiO$_2$ exhibited a high selectivity to C8-aromatics compared to Co1Pt1Sn while Co1Pt1Sn yielded the highest hydrogenolysis reaction at high conversions. In the case of using bimetallic Pt-Sn as the catalyst for n-octane aromatization, it would be a new alternative catalyst because its particle size of metal is decreased; consequently, the coke formation and hydrogenolysis reaction is inhibited. In addition, the PtSn alloy formation caused the electron transfer from tin to platinum atoms; as a result, the OX molecules were more produced leading to a high production of C8-aromatics products.

---

*Being prepared for Journal of Catalysis

6.2 Introduction

Platinum clusters in alkaline LTL zeolite are very efficient for the direct dehydrocyclization of n-hexane into benzene [1-5]. However, they have not been as effective when the feed is n-octane [6,7]. Although Pt/KL catalysts prepared by vapor phase impregnation (VPI) result in very high Pt dispersion and maximum incorporation of Pt inside the channels of the zeolite [8,9], the activity for n-octane aromatization is much lower than that of n-hexane and rapidly drops, compared to the almost total absence of deactivation with the n-hexane feed. The product distribution obtained from the n-octane conversion yielded benzene and toluene as the dominant aromatic compounds, with small quantities of ethylbenzene (EB) and o-xylene (OX), which are the expected products of a direct six membered ring closure. Since the pore size of the KL zeolite is 0.71 nm [10], larger than the critical diameter of EB but smaller than that of OX, OX diffuses much slower than EB. As a result, OX would preferentially convert to benzene and toluene by the secondary hydrogenolysis reaction before escaping from the pore of zeolite.

For the aromatization of n-alkane, there are three different types of hydrogenolysis reaction which are hydrogenolysis of alkane, hydrogenolysis of alkylcyclopentane (ring opening reaction) and hydrogenolysis of alkylcyclohexanes (dealkylation reaction) [11]. In the case of aromatization of n-octane, the dealkylation of alkylcyclohexanes is the prominent reaction observed compared to the ring opening of alkylcyclohexanes or hydrogenolysis of n-octane. Since the rate for hydrogenolysis of n-octane is low and the ring opening of alkylcyclohexanes was limited by the formation of C8-aromatic products. Responsible for this selectivivty loss is hydrogenolysis, a structure sensitive reaction that required large ensembles of platinum atoms [12,13]. By contrast, for n-hexane aromatization occurred on the smallest Pt clusters with minimize hydrogenolysis, since aromatics selectivity will be decreased when Pt clusters are larger due to the enhancing of the hydrogenolysis reaction [14]. In the case of n-octane aromatization, less C8-aromatic products (EB and OX) were obtained because of the secondary hydrogenolysis reaction of both molecules before they diffused out of the pore. There are two possible factors affected on the selectivity of C8 aromatic products. The first ones are the pore length

of KL zeolite [15]. Exxon researchers have observed that Pt/KL zeolites with a very flat cylinder shape (coin or hockeypuck shape), gave greater selectivity and yield of benzene for aromatization of n-hexane [16]. Accordingly, using the shorter channel length KL zeolite might decrease the residence time of both EB and OX inside the pore. As a result, the hydrogenolysis reaction can be inhibited. The second ones are the particle size of the platinum clusters. Over platinum, the hydrogenolysis of alkanes is strongly dependent on the metal particle size. It is now well recognized that the hydrogenolysis activity of Pt decreases substantially when the dimension of the Pt particle is less than 1-2 nm and also when Pt is alloyed with a nonactive metal, such as Au, Sn, Pb [1,12]. For many reactions in the petrochemical industries, such as naphtha reforming, alkane dehydrogenation, n-alkane dehydrocyclization, etc., tin (Sn) was used as a promoter to improve the catalytic activity for such reactions. For example, in the naphtha reforming, tin is added to Pt/Al_2O_3 catalyst and acts as the promoter metal. Tin modifies the stability and selectivity of the Pt function in two ways, which are ensemble and electronic effect. By an ensemble effect, tin decreased the number of contiguous platinum atoms and then the multipoint adsorption of hydrocarbon molecules on the surface is hampered. Consequently, the hydrogenolysis and deactivation by coke deposition can be reduced. In addition to the purely geometric, ensemble dilution, Sn modifies Pt electronically by giving its electron to the holes of 5d band of platinum atom [17-19]. By this electronic effect, C-C bond hydrogenolysis does not occur because the hydrocarbon cannot be strongly adsorbed on the catalyst surface.

Comparison among Pt, Pt-Sn and Pt-W, supported on alumina, $Pt-Sn/Al_2O_3$ is the best catalyst for n-octane reforming since less hydrogenolysis was produced and more isomerization and cyclization were obtained. Tin is the best modifier of the metallic function because it decreases hydrogenolysis and the production of highly dehydrogenated coke precursors [20]. Similarly, for n-heptane conversion, it was found that the addition of tin improved the stability of the Pt/Al_2O_3 catalysts, caused a decrease in the selectivity for hydrogenolysis and increase in the selectivity for aromatization products [21]. In addition, on $Pt-Sn/\gamma-Al_2O_3$, it was observed that the bimetallic Pt-Sn catalyst prepared by simultaneous impregnation as a complex showed higher activity that the catalyst prepared by successive impregnation [22]. In

the case of using the Pt/KL as the catalyst for n-hexane aromatization, it has been found that catalytic performance of the Pt/KL catalyst can be improved with mainly the Pt ensemble effect by an incorporation of tin [23].

For the reforming reaction or aromatization of n-alkane, the hydrogenolysis reaction is inhibited by the addition of Sn. In contrast with those reaction, the addition of tin to Pt/SiO_2 or Pt/L catalysts can enhance the dehydrogenation selectivity for dehydrogenation reaction [24-26]. Therefore, the possibility to produce more aromatics is much more since alkane dehydrocyclization is occurred by a consecutive stepwise dehydrogenation to produce aromatics [11,27,28]. This proposed mechanism is called Triene mechanism. As observed in the previous works [15,29], in the case of n-hexane aromatization, the formation of benzene is preceded by the formation of hexenes. Likewise, for n-octane aromatization, n-octane is dehydrogenated to octenes and then cyclized to produce C8-aromatics. However, the opportunity for occurring the hydrogenolysis or coking reaction is observed since these reactions proceed through the formation of highly dehydrogenated. Therefore, the catalytic activity of the bimetallic Pt-Sn/KL catalyst should be maximized to avoid the formation of hydrogenolysis reaction and coke formation.

In this study, we have investigated the effects of the preparation method of Pt-Sn/KL catalysts and the ratio of Sn/Pt on the n-octane aromatization reaction. Pt was incorporated in the KL zeolites by the vapor phase co-impregnation and vapor phase sequential impregnation. The fresh catalysts were characterized by hydrogen chemisorption, TEM analysis, TPR and XPS. The activity and selectivity of all catalysts in the series for the *n*-octane aromatization were compared at 500°C and atmospheric pressure. The amount of coke deposited on the spent catalysts during reaction was determined by temperature programmed oxidation (TPO). It has been found that addition of Sn can result in a significant improvement in catalytic performance in the conversion of n-octane.

6.3 Experimental

6.3.1 Catalyst Preparation

The bimetallic Pt-Sn/KL catalysts were prepared by vapor phase impregnation (VPI) with three different techniques. One sample was made by co-impregnation. Other series of the catalyst were prepared by vapor phase sequential impregnation of Pt followed by Sn and Sn followed by Pt. For each technique, the nominal percentage of platinum and tin loading is 1 wt%. Prior to impregnation, the KL zeolite (from Tosho company, HSZ-500, $SiO_2/Al_2O_3=6$) was dried in an oven at 110°C overnight and calcined at 500°C in flowing dry air of 100 cm^3/min.g for 5 h. In the case of sequential impregnation of Pt followed by Sn or Sn followed by Pt, the dried support was mixed physically with either weighed platinum (II) acetylacetonate (Alfa Aesar) or tin (IV)bis acetylacetonate dichloride (Aldrich), which is selected as the first metal under nitrogen atmosphere. The mixture was then loaded in a tube reactor before being subjected to a helium flow of 5 cm^3/min.g. The reactor was gradually ramped to 40°C and held for 3 h, and ramped again to 60°C and held for 1 h. After that, it was further ramped to 110°C where the mixture was held for 1 h to sublime the Pt $(AcAc)_2$. After being cooled down to room temperature, it was ramped to 350°C in flowing air for 2 h to decompose the platinum precursor. The resulting materials were stored in the oxidic form. After that, the second metal was loaded using the same technique for loading the first metal. In the case of co-impregnation, the platinum and tin precursors were mixed physically with dried support.

Pt-Sn/SiO$_2$ was prepared by incipient wetness impregnation using SnCl∘2H$_2$O and H$_2$PtCl$_6$∘6H$_2$O as the precursors for metals. Both precursors were loaded on the silica (HilSil 220 was provided from PPG Siam Silica Col, Ltd) by incipient wetness co-impregnation with the 1wt% of Pt and 1 wt% of Sn using HCl as the solvent. Before loading metals, silica was calcined at 400°C. After loading the metal, the impregnated sample was dried overnight at 110°C and calcined at 400°C in the air flow for 2 h.

To study the effect of the amount of tin, the nominal platinum loading was held constant at 1wt%, and the tin loading was varied as described in Table 6.1. In this study, the bimetallic PtSn/KL catalysts were prepared using vapor phase co-impregnation method.

Table 6.1 Characteristic of the catalysts investigated

Catalysts	Pt (wt%)	Sn (wt%)	Molar Pt:Sn ratio	Preparation techniques
1Pt	1	0	1:0	Vapor phase impregnation (VPI)
Co1Pt0.3Sn	1	0.3	1:0.50	Vapor phase co-impregnation (VPCI)
Co1Pt0.6Sn	1	0.6	1:0.99	Vapor phase co-impregnation (VPCI)
Co1Pt1Sn	1	1	1:1.65	Vapor phase co-impregnation (VPCI)
Co1Pt3Sn	1	3	1:4.95	Vapor phase co-impregnation (VPCI)
Seq1Pt1Sn	1	1	1:1.65	Sequential impregnation (Pt before Sn)
Seq1Sn1Pt	1	1	1:1.65	Sequential impregnation (Sn before Pt)
Pt-Sn/SiO2	1	1	1:1.65	Incipient wetness co-impregnation
1Sn	0	1	0	Vapor phase impregnation (VPI)

6.3.2 Catalyst Characterization

6.3.2.1 Hydrogen Chemisorption

The amount of adsorbed hydrogen on all fresh catalysts was measured in a static volumetric adsorption Pyrex system, equipped with a high-capacity pump that provided a vacuum on the order of 10^{-9} Torr. Prior to each experiment, 0.5 g of dried fresh catalyst was reduced in situ at 500°C for 1 h under flowing H_2, evacuated to at least 10^{-7} Torr at 500°C for 40 min, and then cooled down to room temperature under vacuum. Adsorption isotherms were obtained with several adsorption points ranging from 0 to 50 Torr. The H/Pt values were obtained directly by extrapolating to zero pressure.

6.3.2.2 Transmission Electron Microscopy (TEM)

The TEM images of the catalysts were acquired in a JEOL JEM-2000FX electron microscope. The pre-reduced catalyst samples were ultrasonicated for 5 min in isopropanol until a homogeneous suspension was formed. In each determination, one drop of this mixture was placed over a TEM copper grid and subsequently dried before the analysis.

6.3.2.3 Temperature Programmed Reduction (TPR)

Temperature programmed reduction was performed on the fresh catalysts. For each run, the samples were weighed 50 mg. TPR runs were

conducted using a heating rate of 10°C/min in a flow of 5%H_2/Ar (30 cc/min) up to 900°C. The ice trap was used to eliminate water during the operation.

6.3.2.4 X-Ray Photoelectron Spectroscopy (XPS)

XPS data were achieved on a Physical Electronics PHI 5800 ESCA system using monochromatic Al K$_{ı́A}$ excitation (1486.6 eV) with an energy resolution of 125 meV under a background pressure of approximately $2.0 ı́ß 10^{-9}$ Torr. The electron takeoff angle was 45° with respect to the sample surface, and pass energy of 23 eV was typically used for the analysis. The energy scale of the instrument was calibrated using the Ag $3d_{5/2}$ line at binding energy of 368.3 eV. The binding energy values reported below are all referenced to the Fermi level. Quantification of the surface composition was carried out by integrating the peaks corresponding to each element with aid of the Shirley back ground subtraction algorithm, and then converting these peak areas to atomic composition by using the sensitivity factors provided for the each element by the PHI 5800 system software. The reduction treatment was carried out under a hydrogen flow at 500°C for 1 h. After that, the sample was transferred into the XPS holder under a He flow to avoid any contact with air.

6.3.2.5 Temperature Programmed Oxidation (TPO)

This technique was employed to analyze the amount and characteristics of the coke deposited on the catalysts during reaction. TPO of the spent catalysts was performed in a continuous flow of 2%O_2 in He while the temperature was linearly increased with a heating rate of 12°C/min. The oxidation was conducted in a ¼ in. quartz fixed-bed reactor after the spent catalyst had been dried at 110°C overnight, weighted (0.030 g), and placed between two layers of quartz wool. The sample was further purged at room temperature by flowing 2% O_2 in He for 30 min before the TPO was started. The CO_2 produced by the oxidation of the coke species was converted to methane using a methanizer filled with 15% Ni/Al_2O_3 and operated at 400°C. The evolution of methane was analyzed using an FID detector.

6.3.3 Catalytic Activity

The catalytic activity studies were conducted at atmospheric pressure in a ½ inch diameter glass tube reactor equipped with an internal K-type thermocouple for temperature measurements. In the continuous-flow reactor 0.2 g of fresh catalyst was used in each run. Prior to reaction, the catalyst was slowly ramped in flowing H_2 for 2 h up to 500°C and in-situ reduced at that temperature for 1 h. The n-octane feed was continuously injected from a syringe pump, keeping in all the experiments a hydrogen to n-octane molar ratio of 6:1. The products were analyzed by gas chromatography using a Shimadzu 17A-GC equipped with an HP-PLOT/Al_2O_3 "S" deactivated capillary column. The GC column temperature was programmed to obtain an adequate separation of the products. The temperature was first kept constant at 40°C for 10 min and then, linearly ramped to 195°C and held for 30 min.

6.4 Results and Discussion

6.4.1 Characterization of the Fresh Catalysts

Table 6.1 shows the series of the bimetallic Pt-Sn/KL catalysts prepared by different preparation methods and Pt/Sn ratios. To determine the behavior of tin, the bimetallic Pt-Sn/KL catalysts were characterized by TEM, TPR, hydrogen chemisorption, and XPS. TEM images and histogram of particle size distribution obtained by TEM images and histogram of particle size distribution obtained by TEM of the mono- and bimetallic Pt-Sn/KL catalysts were depicted in Figure 6.1. The results showed that the addition of tin enhances the dispersion of metal and also decreases the particle size of metal compared with the Pt/KL catalyst without employing tin. The average particle size of the metal was reported in Table 6.2. It was found that the metal size was decreased to less than 2 nm for the bimetallic Pt-Sn catalysts prepared by different methods at Sn/Pt ratio of 1. However, there are some parts of metal clusters which have a larger particle size than 2 nm for such catalysts as observed in the histogram. In addition, it was observed that the higher the amount of tin, the more the reducing in the particle size of metal

as observed in the Co1Pt0.3Sn, Co1Pt0.6Sn, and Co1Pt1Sn. For aromatization of n-alkane using a monofunctional catalyst, KL zeolite was used as the support because the Pt cluster can disperse well on this zeolite compared with using SiO_2 as the support. Therefore, to determine that the good dispersion of metal on bimetallic Pt-Sn catalyst is due to using KL as the support or due to the addition of tin, $Pt-Sn/SiO_2$ was prepared to study. It was observed that the metal clusters are dispersed well on the silica support; in addition, the particle size is decreased as observed on the bimetallic Pt-Sn/KL catalysts. Therefore, the addition of tin causes the decreasing in the particle size of the metal; consequently, the metal is dispersed well.
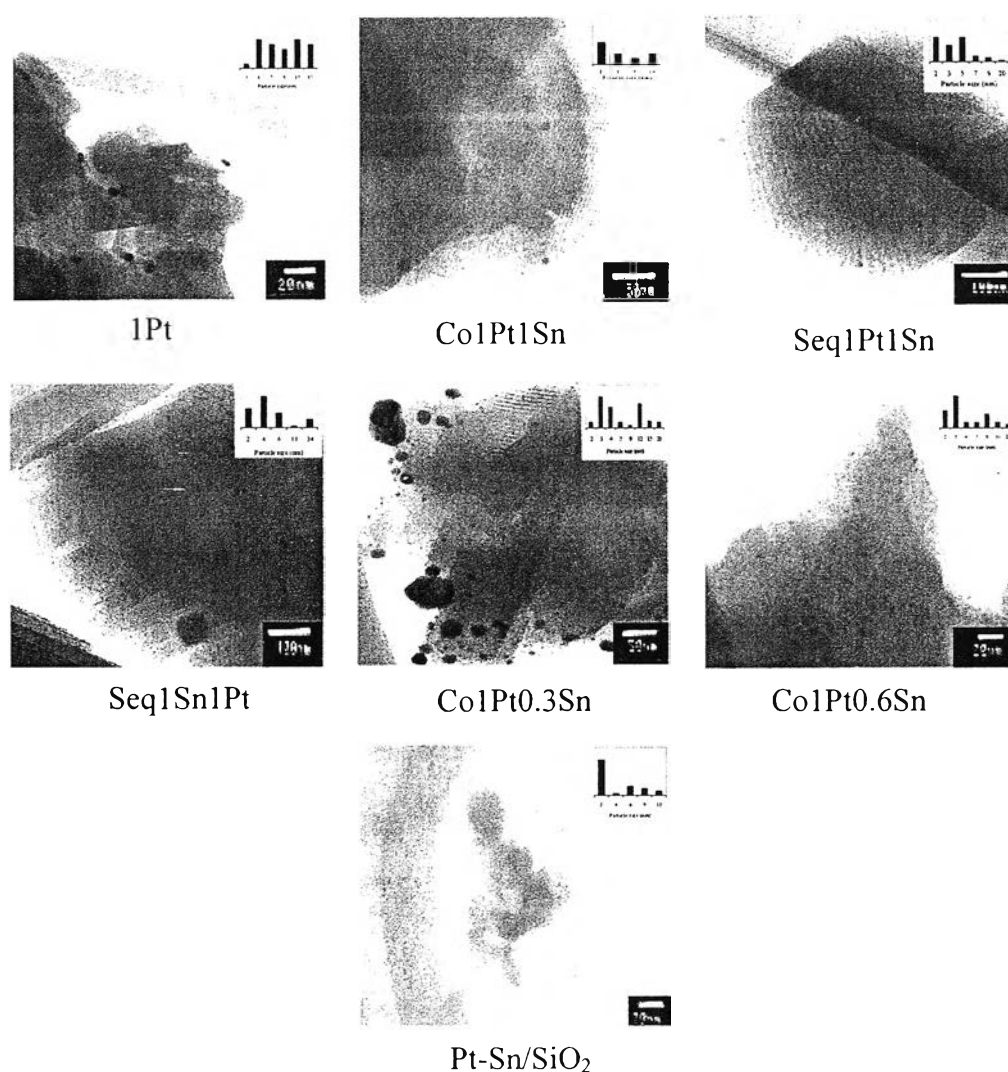
Figure 6.1 TEM images and histograms of particle size distribution obtained by TEM of the bimetallic Pt-Sn catalysts.

Table 6.2 Analysis of fresh catalysts

Catalysts	Pt (wt%)	Sn (wt%)	H/Pt ratio after reduction at 500°C	Average particle size (nm) (measured from TEM)	Coke deposited after reaction 550 min time on stream (wt%)
1Pt	1	0	1.77	6.91-13.06	2.21
Co1Pt0.3Sn	1	0.3	1.50	2.51-3.51	2.90
Co1Pt0.6Sn	1	0.6	1.24	1.69-2.52	2.70
Co1Pt1Sn	1	1	0.13	1.93-3.40	2.18
Seq1Pt1Sn	1	1	0.27	1.65-4.01	2.12
Seq1Sn1Pt	1	1	1.34	1.94-4.89	0.94
Pt-Sn/SiO$_2$	1	1	0.11	1.59	0.39

To investigate the reducibility of samples, a TPR study was carried out. Figure 6.2(a) and 6.2(b) showed the TPR profiles of the mono- and bimetallic Pt-Sn/KL catalysts. For the monometallic 1Pt catalyst, a broad reduction peak is centered at 210°C which is represented to the reduction of Pt (IV) to Pt^0 [30-32]. The temperatures are higher than those reported for bulk precursor [32]. On the other hand, the TPR of 1Sn shows one broad reduction peak starting at 300°C with the maximum around 420°C. When the profiles of the two monometallic catalysts 1Pt and 1Sn are combined, the sum does not match the profile of the bimetallic Pt-Sn/KL catalysts. Firstly, in consideration of the profile of Pt-Sn/SiO$_2$, there is only one sharp peak at 264°C since there is a homogeneous PtSn alloy observed on this catalyst. Meanwhile, the TPR profiles of bimetallic Pt-Sn/KL catalysts, which are Co1Pt0.3Sn, Co1Pt0.6Sn, Co1Pt1Sn, Seq1Pt1Sn, and Seq1Sn1Pt, have the broad peak which can be deconvoluted into three peaks. There are TPR profiles of Pt (IV) to Pt^0 (Pt rich phase), PtSn alloy, and Sn rich phase as reported in Table 6.3. From these data, Co1Pt1Sn exhibited the high fraction of PtSn alloy phase compared to other bimetallic Pt-Sn/KL catalysts. Whereas, Co1Pt0.3Sn and Co1Pt0.6Sn showed high fraction of Pt rich phase and Sn rich phase compared to others. However, the Pt rich phase is decreased with the increasing amount of tin. The combined TEM and TPR results indicated that alloy formation causes the decreasing of the particle size of the metal. Nevertheless, some Pt or Sn rich phases were observed in the bimetallic Pt-Sn/KL catalysts; therefore, some larger particle sizes of metal remained.
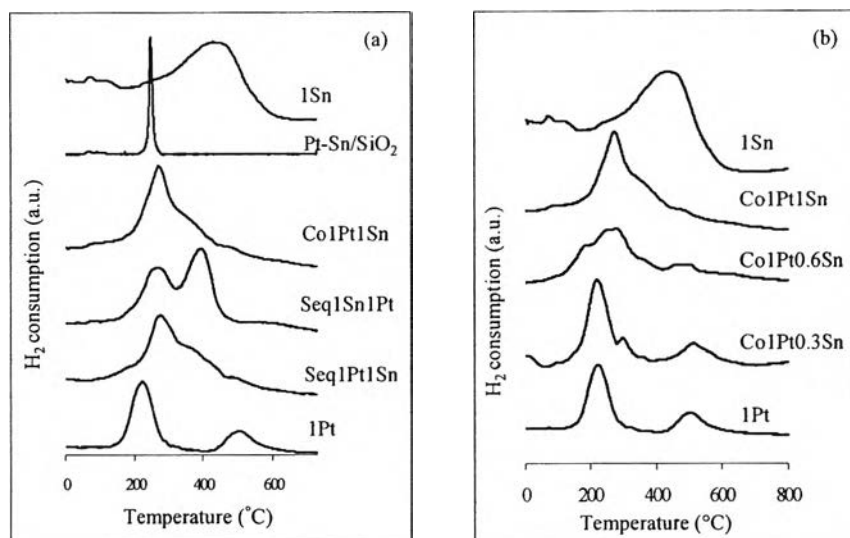
Figure 6.2 TPR profiles of (a) the bimetallic Pt-Sn catalysts prepared by different preparation methods at the ratio of Sn/Pt= 1 and (b) the different Sn/Pt ratios prepared by vapor-phase co-impregnation method.

Table 6.3 Deconvolution of TPR profile of bimetallic catalysts

Catalysts	Area of each TPR temperature (%)		
	150-220°C Pt rich phase	180-280°C Alloy phase of PtSn catalyst	360-520°C Sn rich phase
Co1Pt0.3Sn	64.64	0	34.38
Co1Pt0.6Sn	18.50	42.55	38.95
Co1Pt1Sn	9.39	52.33	38.28
Seq1Pt1Sn	8.70	47.97	43.33
Seq1Sn1Pt	8.16	39.66	52.18

The results of the hydrogen chemisorptions are reported in Table 6.2; the monometallic 1Pt catalyst shows a high H/Pt ratio compared to the bimetallic Pt-Sn catalysts. Therefore, addition of tin caused a strong decrease in the H/Pt ratio. It was found that the decreasing of the H/Pt ratio of the bimetallic Pt-Sn catalysts depends on the fraction of alloy formation. This demonstrated that the addition of tin obviously depressed the availability of surface Pt atoms due to the PtSn alloy formation [32,32-36].

X-ray photoelectron spectra of the Pt4f and Sn3d levels were recorded in order to obtain information about the oxidation states of the metal phased (Pt and/or Sn) on the surface. The peak positions have been corrected for sample charging by using the Si2p peak as a standard at 102.0 eV. Figure 6.3(a) and 6.3(b) showed the Pt4f XPS spectra of the mono- and bimetallic catalysts. In the case of the monometallic 1Pt catalyst, it was found that there were two overlapping signals detected at 70.2 and 72.5 eV, corresponding to Pt^0 and PtO, respectively [37]. However, the third signal is observed in the XPS spectra of the bimetallic Co1PtSn, Seq1Pt1Sn and Pt-Sn/SiO$_2$ catalyts. This signal is located at a binding energy of 69.0 eV, indicating that the presence of tin in the catalysts affects the electronic environment of the platinum by gaining some electron density from tin [3535,38]. Whereas, there are no third signals observed on Seq1Sn1Pt, Co1Pt0.3Sn and Co1Pt0.6Sn due to less PtSn alloy formation. Figure 6.4(a) and 6.4(b) show the Sn3d XPS spectra for the monometallic 1Sn and bimetallic Co1Pt1Sn, Seq1Pt1Sn, Seq1Sn1Pt, Pt-Sn/SiO$_2$, Co1Pt0.3Sn and Co1Pt0.6Sn catalysts. The peak due to metallic tin is found at 484.3 eV, and the peak due to tin oxides is present at 485.8 eV [33,39]. However, it cannot tell the difference between Sn(II) oxide and Sn(IV) oxide from XPS. For the 1Sn catalyst, there is a signal observed at 486.24 eV which corresponds to SnO and/or SnO$_2$. For the XPS spectra of bimetallic catalysts, Co1Pt0.3Sn, Co1Pt0.6Sn, Co1Pt1Sn, Seq1Pt1Sn, Seq1Sn1Pt and Pt-Sn/SiO$_2$, Sn3d peaks were found at 484.7 and 486.9 eV binding energy which represented Sn^0 and Sn(II) and/or Sn(IV), respectively. However, the signal is not shifted toward higher binding energies due to transformation of some electron from tin to platinum as reported by Morales et al. [38]. Nevertheless, it was observed that the bimetallic Pt-Sn/KL catalysts exhibited the different fractions of metallic tin, as shown in Table

6.4. It was found that all or part of metallic tin could be alloyed with platinum to give PtSn alloy [32,35]. The combined TPR and XPS data from the bimetallic Pt-Sn/KL catalysts showed that the higher the fraction of PtSn alloy formation, the higher the metallic tin was observed, as shown in Table 6.4. Some researcher reported that the degree of metallic tin corresponds to a decrease in the particle size of metal: the smaller the particle size of the catalyst, the higher the ratio of alloyed tin. These findings could be explained by assuming that platinum is alloyed with tin or even electronically modified by the tin presence [26,40]. In this work, it was only found that the PtSn alloy formation causes the decreasing of the particle size of metal compared to no alloy formation. However, there is correlation between the degrees of metallic tin with the decreasing of the particle size of metal, as found in the series of Co1Pt0.3Sn, Co1Pt0.6Sn, and Co1Pt1Sn.
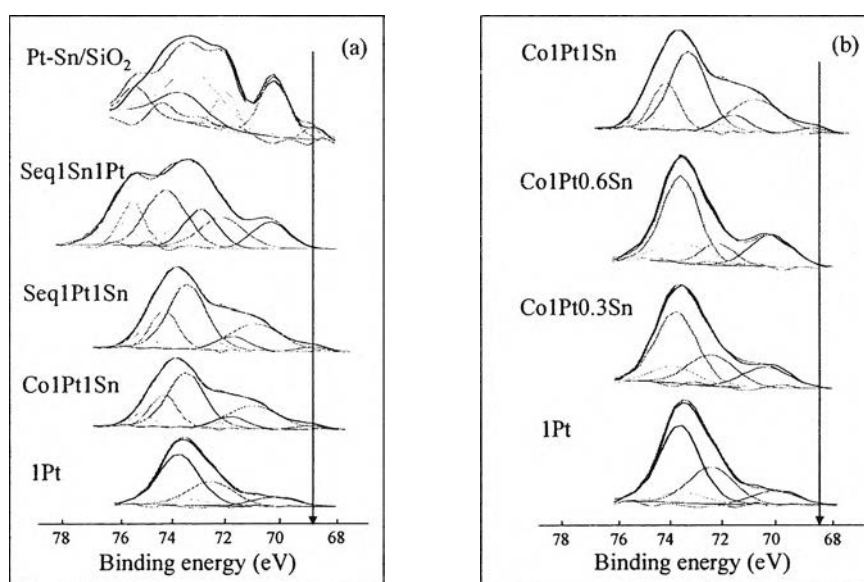
Figure 6.3 Pt4f XPS spectra of (a) the bimetallic Pt-Sn catalysts prepared by different methods at the ratio of Sn/Pt= 1 and (b) the different Sn/Pt ratios prepared by vapor-phase co-impregnation method.
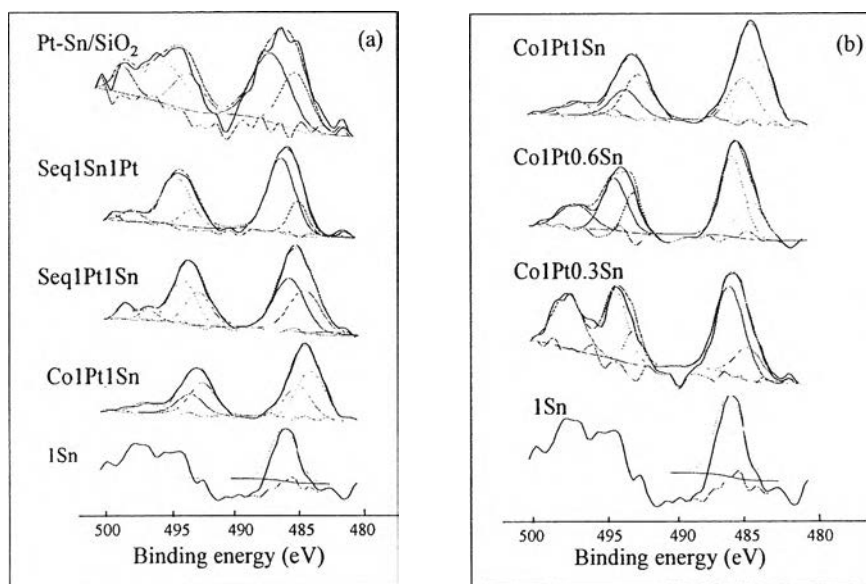
Figure 6.4 Sn3d XPS spectra of (a) the bimetallic Pt-Sn catalysts prepared by different methods at the ratio of Sn/Pt= 1 and (b) the different Sn/Pt ratios prepared by vapor-phase co-impregnation method.

Table 6.4 XPS binding energies

Catalysts	Si2p[a]	Sn3d$_{5/2}$[b]	The fraction of PtSn alloy (%)	Average particle size (nm) (measured from TEM)
1Pt	102	-	0	6.91 - 13.06
Co1Pto.3Sn	102	484.57 (26) 486.93 (74)	0	2.51 - 3.51
Co1Pt0.6Sn	102	484.72(34) 486.06 (66)	42.55	1.69 - 2.52
Co1Pt1Sn	102	484.25 (59) 485.22-486.11 (41)	52.33	1.93 – 3.40
Seq1Pt1Sn	102	484.76 (44) 485.95 (56)	47.97	1.65 - 4.01
Seq1Sn1Pt	102	485.12 (23) 486.45 (77)	39.66	1.94 - 4.89
Pt-Sn/SiO$_2$	102	485.06 (40) 486.93 (60)	100	1.59
1Sn	102	486.24 (100)	0	-

[a] Values reported in eV, and reference to a value of Si2p – 102 eV.

[b] Values in parentheses indicate the percentage of the species.

6.4.2 Catalytic Activity Testing: n-Octane Aromatization
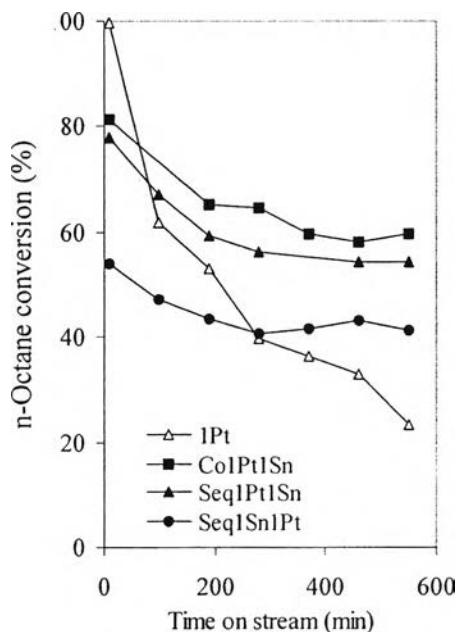
6.4.2.1 The Effect of the Addition of Tin (Sn)

Figure 6.5 The variation of n-octane conversion with time on stream of different prepared bimetallic Pt-Sn/KL catalysts at the ratio of Sn/Pt = 1; reaction conditions: temperature = 500°C, pressure = 1 atm, WHSV = 5 h^{-1}, and H$_2$:HC = 6:1.

Figure 6.5 shows the evolution of n-octane conversion for the mono- and bimetallic catalysts. It was found that the presence of the promoter (Sn) caused a decrease in the initial activity due to the decrease in the platinum adsorption capacity as measured by hydrogen chemisorption [21], but the bimetallic Pt-Sn/KL catalysts showed better stabilities than the monometallic 1Pt catalyst. 1Pt exhibited a rapid deactivation due to coke plugging inside the pores because of the restricted diffusion out of the pore of C8-aromatic products (EB and OX) [15]. Many researcher proposed that tin promoted the stability of the catalysts by inhibiting the formation of highly dehydrogenated surface species which are the intermediate for coke formation [21,25,26,41]. This change of bond strength between chemisorbed hydrocarbons and Pt surface atoms is due to electron transfer from the promoter to Pt (electronic effect), as observed from the XPS data. Moreover, TEM results showed the decreasing of the metal size. Therefore, the

promoter presence hinders the adsorption of these molecules on the metal atoms, and the coke precursors are drained to the support surface, leaving the metal surface available for reaction because the coke precursors are relatively large and also demand large ensembles for adsorption [21]. In the case of each bimetallic Pt-Sn/KL catalysts prepared by different preparation methods, it was found that the stability and the activity of the catalysts corresponded to the fraction of PtSn alloy phase formation. As a result, Co1Pt1Sn exhibited better stability and activity than the others. As reported by Stagg et al. [42], in choosing a preparation method, one needs to maximize the degree of Pt-Sn interaction rather than maximize the metal dispersion because the fraction of alloyed Pt is the one that will be responsible for the sustained activity. Somehow, it was observed that even though the stability of the Co1Pt1Sn and Seq1Pt1Sn, was improved, the amount of coke deposited is similar to 1Pt, except for Seq1Sn1Pt as reported in Table 6.2.

In term of aromatic product selectivity as shown in Figure 6.6(a) and 6.6(b), the results showed that Co1Pt1Sn and Seq1Pt1Sn yielded high selectivity to total aromatics and C8-aromatics selectivity compared to Seq1Sn1Pt and 1Pt. As shown in Table 6.5, the predominant aromatic products on both Co1Pt1Sn and Seq1Pt1Sn are C8-aromatics (EB and OX) with the small amount of benzene and toluene, which are undesired products from the hydrogenolysis reaction. In addition, even though Seq1Sn1Pt gave lower total aromatic selectivity than 1Pt, the major products are still C8-aromatic products. Hence, the addition of tin causes a decrease in the hydrogenolysis products and increase in C8-aromatic products. In the consideration of the results from TEM, it can be proposed that tin inhibited the hydrogenolysis reaction by dilution of the Pt metals into small ensembles. Therefore, the hydrogenolysis, which is a more sensitive reaction to bigger ensembles, is shifted to dehydrocyclization, which requires smaller ensembles. Moreover, combination the results from XPS and TPR, it was believed that tin decreased the hydrogenolysis reaction by the electronic effect since some electrons of tin were transferred to Pt when PtSn alloy phase was formed. Consequently, C-C bond hydrogenolysis does not occur because the hydrocarbon cannot be strongly adsorbed on the catalyst surface. Not only the hydrogenolysis reaction is decreased by electronic effect, but also the enhancement of OX molecules as shown in Table

6.5 is due to electronic effect. Westfall et al. [43] and Lee et al. [44] informed that the mole ratio of EB/OX may be an indirect index, indicating the electron density of Pt by the addition of tin. Dehydrocyclization of n-octane produced EB and OX by a mechanism that involves the direct formation of a six-member carbon ring [45]. The bond strength of primary hydrogen in $-CH_3$ is only greater than that of secondary hydrogen in $-CH_2$. Therefore, it was expected that the 6-membered rind intermediate would lead to an almost equal amount of EB and OX [1]. However, tin would alter the ability of Pt to rupture the C-H bond and favor the rupture of the weaker C-H bond of the secondary hydrogens of the $-CH_2$ groups over those of the primary hydrogen of the $-CH_3$ groups. Therefore, the EB/OX ratio is decreased when tin was employed. From Table 6.5, it was found that the EB/OX ratio of 1Pt is higher than that of Co1Pt1Sn and Seq1Pt1Sn due to no electrons being transferred from tin to Pt atom.
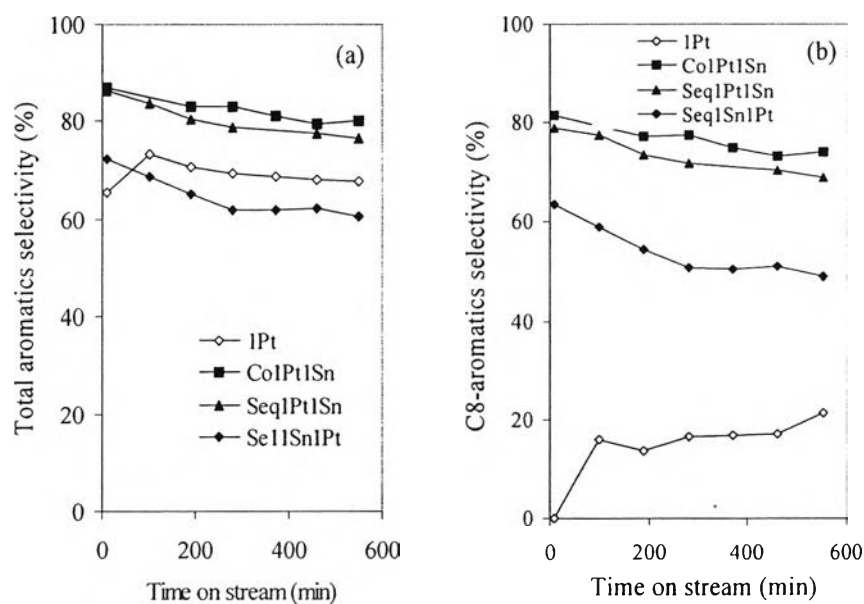

Figure 6.6 The variation of (a) total aromatics selectivity and (b) C8-aromatics selectivity with time on stream of different preparation bimetallic Pt-Sn/KL catalysts at the ratio of Sn/Pt = 1; reaction conditions: temperature = 500°C, pressure = 1 atm, WHSV = 5 h^{-1}, and H_2:HC = 6:1.

Table 6.5 Properties of different prepared bimetallic Pt-Sn/KL catalysts tested for n-octane aromatization after 550 min time on stream; reaction condition: temperature = $500^{\circ}C$, pressure = 1 atm, WHSV = 5 h^{-1}, and H_2:HC = 6:1

Properties	1Pt	Co1Pt1Sn	Seq1Pt1Sn	Seq1Sn1Pt	Pt-Sn/SiO$_2$	Co1Pt1Sn*	Pt-Sn/SiO$_2$*	Pt/SiO$_2$**
Conversion (%)	23.28	59.51	54.20	41.24	56.89	97.91	91.20	16.80
Product distribution (%)								
C1-C5	19.72	1.91	2.10	2.78	1.94	10.38	2.71	7.1
Total enes (C6-C8enes)	12.40	17.85	21.45	36.51	30.43	0.90	9.16	43.7
Total aromatics	67.88	80.25	76.45	60.71	67.63	60.17	88.13	48.80
Total aromatics (%)								
Benzene	19.05	0.39	0.40	0.39	0.00	6.83	0.00	0.00
Toluene	27.59	5.78	7.06	11.46	0.00	21.39	0.00	0.00
EB	13.95	29.88	27.89	21.74	25.29	18.23	28.60	21.50
m-.p-Xylene	1.82	0.45	0.26	1.34	1.38	3.51	4.47	1.60
o-Xylene	5.47	43.74	40.85	25.79	40.96	38.43	47.31	24.80
EB/OX ratio	2.55	0.68	0.68	0.84	0.62	0.47	0.60	0.87
Hydrogenolysis products	66.36	8.08	9.56	14.62	1.94	38.61	2.71	7.1

*The data were obtained at the WHSV of 1.5 h^{-1} and 30-min time on stream.
**The data were obtained from previous work: S.Jongpatiwut et al., J.Catal. 218, 1 (2003).

In the case of Seq1Sn1Pt, even though the particle size of metal is decreased, the selectivity to OX molecules does not improve as much as observed on Co1Pt1Sn and Seq1Pt1Sn. However, the selectivity to EB molecules is almost similar. The combined results from TPR and XPS showed that Seq1SnsPt has less PtSn alloy formation and no electron transfer from tin to platinum atoms. Therefore, the selectivity to OX molecules is not improved as much as observed on Co1Pt1Sn and Seq1Pt1Sn. In fact, product ratio of EB/OX is about unity, as observed over Pt/SiO$_2$ and other nonmicroporous catalysts [6]. On the other hand, the EB/OX ratio becomes greater than 1 when there is pore restriction and it gets greater as the diffusional effects become more pronounced, for example by carbon deposition. Since the critical size of the OX molecule is larger than that of EB, then the speed of transport through the pores is slower for OX than for EB; therefore, OX is more easily converted to smaller molecules, such as benzene, toluene, and methane, by secondary hydrogenolysis. Consequently, the EB/OX ratio is greater than 1. As shown in Table 6.5, the EB/OX ratio obtained from using Seq1Sn1Pt as the catalyst is 0.84, which is almost one. Therefore, the hydrogenolysis reaction, which takes place inside the pore, is hampered due to the effect of dilution of Pt into small ensembles. However, electronic effect is also important for decreasing the hydrogenolysis reaction, as shown in Table 6.5. For each different preparation method of the bimetallic Pt-Sn/KL catalysts, even though the particle size of the metal is decreased by the addition of tin, Co1Pt1Sn still exhibited less hydrogenolysis products compared to Seq1Pt1Sn and Seq1Sn1Pt due to high fraction of PtSn alloy phase. Therefore, both geometric and electronic effects are important factors on the catalytic activity in the aromatization of n-octane for inhibition of hydrogenolysis reaction and enhancement in C8-aromatics. In contrast, it was observed that geometric factor was an important parameter on the catalytic activity in the dehydrocyclization of n-octane, whereas, the electronic factor was that in the aromatization of n-hexane over Pt-Sn/γ-Al$_2$O$_3$ [22].

Pt-Sn/SiO$_2$ was used to study further how the importance of geometric and electronic effects is on aromatization of n-octane. From previous work [6], it was found that Pt/SiO$_2$ catalyst is less active than Pt/KL for n-octane aromatization because of low dispersion of this catalyst. However, less secondary

hydrogenolysis reaction was observed on Pt/SiO_2 compared with that observed on Pt/KL catalyst due to lack of the effect of pore restriction. It was found that the addition of tin improved the activity and stability of the catalysts compared to Pt/SiO_2 as shown in Table 6.5. However, the activity of $Pt-Sn/SiO_2$ is less than that of Co1Pt1Sn as shown in Figure 6.7(a). This behavior is similar to the results observed from the aromatization of n-hexane and n-octane [6] because of the unique properties of Pt/KL catalysts as proposed by several researchers [1,3,4,5]. Consequently, the selectivity to C8-aromatics obtained from $Pt-Sn/SiO_2$ is less than that obtained from Co1Pt1Sn as depicted in Figure 6.7(b). However, the stability of Co1Pt1Sn is similar to that of $Pt-Sn/SiO_2$ because tin inhibited the formation of highly dehydrogenated surface species which are the intermediate for coke formation. The addition of tin on Pt/SiO_2 improves the selectivity to OX molecules due to the electronic effect as observed on Co1Pt1Sn. Therefore the EB/OX ratio is decreased from 0.87 to 0.62 as shown in Table 6.5.
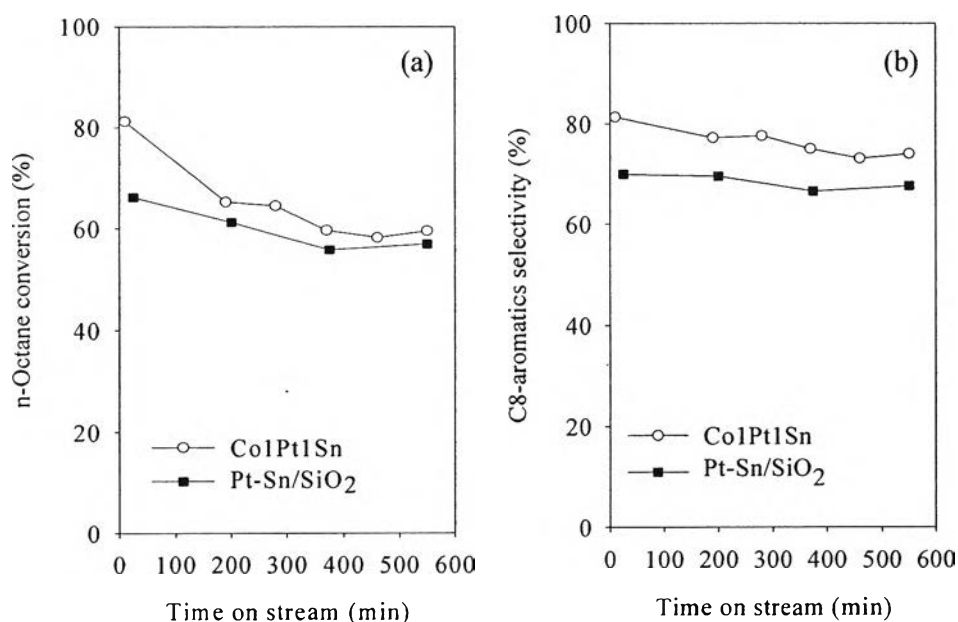
Figure 6.7 The variation of (a) n-octane conversion and (b) C8-aromatics selectivity with time on stream of Co1Pt1Sn and Pt-Sn/SiO2; reaction conditions: temperature = 500°C, pressure = 1 atm, WHSV = 5 h^{-1}, and H$_2$:HC = 6:1.

To study the importance of the pore of KL zeolite, the plot between the C8-aromatics selectivity with n-octane conversion of 1Pt, Co1Pt1Sn, and Pt-Sn/SiO$_2$ at low conversion was introduced as shown in Figure 6.8. The results showed that no difference in selectivity to C8-aromatics was observed at low conversion between Co1Pt1Sn and Pt-Sn/SiO$_2$. However, Pt-Sn/SiO$_2$ exhibited high selective to C8-aromatics compared to Co1Pt1Sn at high conversion. Since the aromatization was occurred by Triene mechanism [11,12], therefore there are high selectivity to alkenes at the low conversion. The advantage for using KL zeolite as the support is to easily cyclize of alkenes to aromatics [1] compared to using silica which is non-microporous as the support. It was found that Pt-Sn/SiO$_2$ has the ability to produce more alkenes product than Co1PtSn and 1Pt as shown in Figure 6.9(a). Therefore, Pt-Sn/SiO$_2$ should give low ability to produce aromatics at low conversion compared to Co1Pt1Sn. However, the hydrogenolysis reaction was more pronounced on Co1Pt1Sn and 1Pt as shown in Figure 6.9(b). This might result in low C8-aromatics products and no difference in C8-aromatics selectivity at low conversion between Co1Pt1Sn and Pt-Sn/SiO$_2$. However, to ignore the effect of dehydrogenation reaction, the conversion of both Co1Pt1Sn and Pt-Sn/SiO$_2$ is maximized to 98% and 91%, respectively. It was found that Pt-Sn/SiO$_2$ exhibited more selectivity to EB and OX molecules than Pt/KL as shown in Table 6.5. In addition, it showed that a large amount of hydrogenolysis products which are benzene, toluene, C1-C5 were observed on Pt/KL catalysts at high conversion. Since there is pore geometric effect for diffusion of C8-aromatics out of the KL zeolite pore, those molecules are converted to smaller molecules by hydrogenolysis reaction. In contrast there is no pore geometric effect on Pt-Sn/SiO$_2$. Therefore at the high catalytic activity, Pt-Sn/SiO$_2$ could be the effective catalyst for n-octane aromatization when there is perfect PtSn alloy formation. As a result, the pore of KL zeolite is not necessary to inhibit coke formation, since addition of tin resulted in small particles size of metal so that the cracking and hydrogenolysis reaction were shifted to a favorable dehydrocyclization.

In addition, it was found that less coke formation was produced on Pt-Sn/SiO$_2$ compared to the bimetallic Pt-Sn/KL catalysts as shown in Table 6.2. On both the bimetallic Pt-Sn/KL and Pt-Sn/SiO$_2$ catalysts, the coke

formation is inhibited by both geometric and electronic effects. However, less coke formation is observed on Pt-Sn/SiO₂.
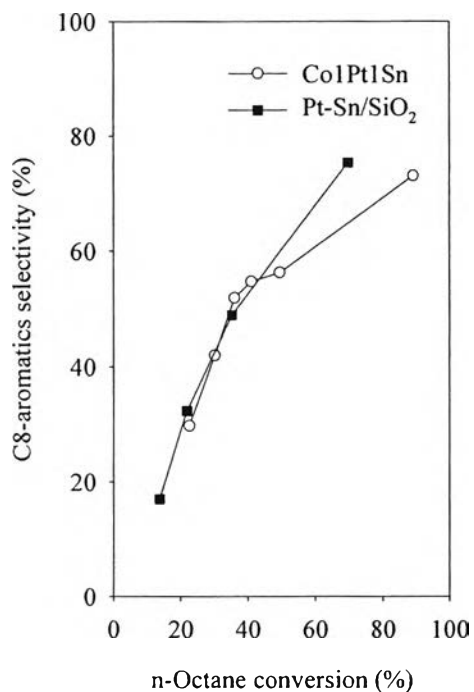

Figure 6.8 The variation C8-aromatics selectivity with n-octane conversion of Co1Pt1Sn and Pt-Sn/SiO₂; reaction conditions: temperature = 500°C, pressure = 1 atm, WHSV = 0.5-5 h⁻¹, and H₂:HC = 6:1.
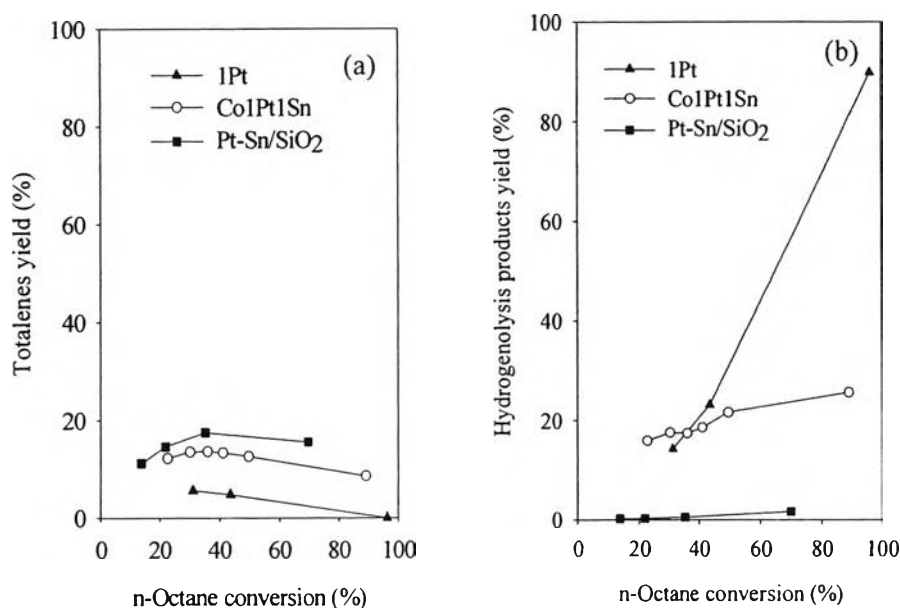
Figure 6.9 The variation of (a) totalenes yield and (b) hydrogenolysis product yield with n-octane conversion of 1Pt, Co1Pt1Sn and Pt-Sn/SiO$_2$; reaction conditions: temperature = 500°C, pressure = 1 atm, WHSV = 0.5-5 h^{-1}, and H$_2$:HC = 6:1.

6.4.2.2 The Effect of Sn/Pt Ratio

To study the effect of Sn/Pt ratio, Co1Pt0.3Sn, Co1Pt0.6Sn, Co1Pt1Sn and Co1Pt3Sn were selected for studying. Figure 6.10 showed the evolution of n-octane conversion for these catalysts as a function of time on stream. The results showed that the activity of the catalyst is increased with increasing the Sn/Pt ratio. From TPR analysis, it was found that the higher the amount of tin, the lower the amount of Pt rich phase. Consequently, there is higher fraction of PtSn alloy phase observed as increasing the amount of tin. Therefore, the activity of both Co1Pt0.3Sn and Co1Pt0.6Sn is lower than that of Co1Pt1Sn which has a high fraction of alloy formation compared with those catalysts. From TEM image, the particle size of metal is decreased with the increased Sn/Pt ratio. Therefore, activity of Co1Pt1Sn is improved by geometric and electronic effect. As shown in Table 6.2, the amount of coke deposited decreased with increasing the Sn/Pt ratio. In addition, from TPO profiles described in Figure 6.14, it was found that the temperature of oxidation of coke deposited was reduced as increasing in Sn/Pt ratio. Therefore, it can imply that tin changes the type of coke formation. However, the activity of the

bimetallic Pt-Sn/KL is decreased when excess amount of Sn was added. As shown in Figure 6.10, the activity of Co1Pt3Sn is less than the others because the excess amount of tin might cover the active site; consequently, the activity is decreased.
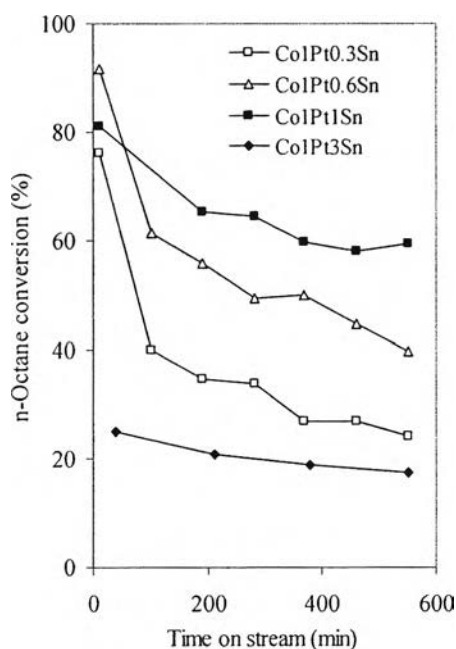

Figure 6.10 The variation of n-octane conversion with time on stream of various Sn/Pt ratios of the bimetallic Pt-Sn/KL catalysts prepared by vapor phase co-impregnation; reaction conditions: temperature = 500°C, pressure = 1 atm, WHSV = 5 h⁻¹, and H₂:HC = 6:1.

In terms of product selectivity, Co1Pt1Sn exhibited high selectivity to total aromatics and C8-aromatics compared with Co1Pt0.3Sn, Co1Pt0.6Sn, and Co1Pt3Sn as shown in Figure 6.11(a) and 6.11(b). The major aromatic products are C8-aromatics. Increasing the amount of tin improves selectivity to C8-aromatics by geometric and electronic effect. However, less selectivity to total aromatics and C8-aromatics was observed when excess amount of tin was added. By geometric effect, in which a physical dilution by tin takes place, the presence of tin decreased the size of the metal as shown in TEM image so that hydrocarbon cannot readily form multiple carbon-metal bonds. C-C bond hydrogenolysis does not occur, as a result, less benzene selectivity was observed on

Co1Pt1Sn as shown in Figure 6.12. By electronic effect, the hydrocarbon cannot be strongly adsorbed on the catalyst surface; consequently, C-C bond hydrogenolysis does not occur. Moreover, tin enhanced the ability to break the $-CH_2$ bond and yield high production of OX molecules compared to EB molecules. As a result, the EB/OX ratio is decreased as the Sn/Pt ratio is increased as shown in Figure 6.13. However, the EB/OX ratio was increased when Sn/Pt ratio is higher than 1 because this catalyst is less active and selective to aromatic products. Therefore, no catalytic performance of the bimetallic Pt-Sn/KL catalyst was improved by electronic effect.
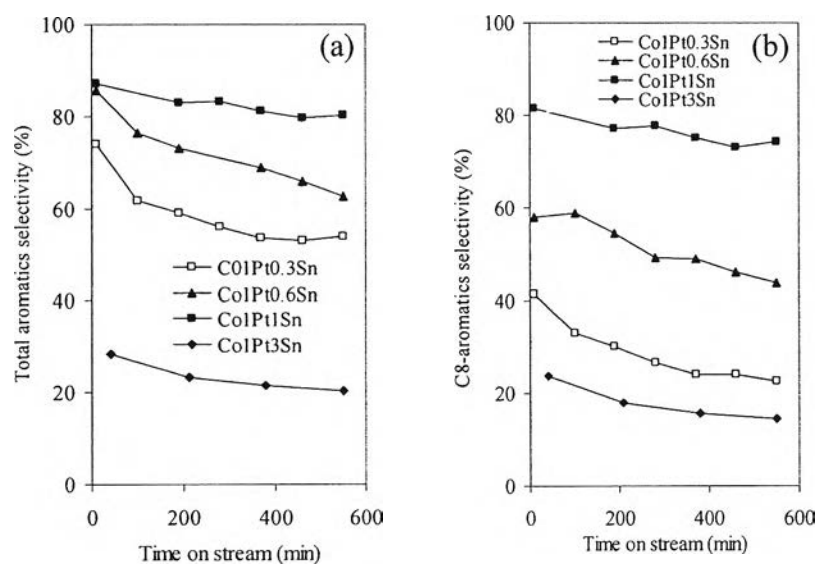
Figure 6.11 The variation of (a) total aromatics selectivity and (b) C8-aromatics selectivity with time on stream of various Sn/Pt ratios of the bimetallic Pt-Sn/KL catalysts prepared by vapor phase co-impregnation; reaction conditions: temperature = 500°C, pressure = 1 atm, WHSV = 5 h^{-1}, and H_2:HC = 6:1.
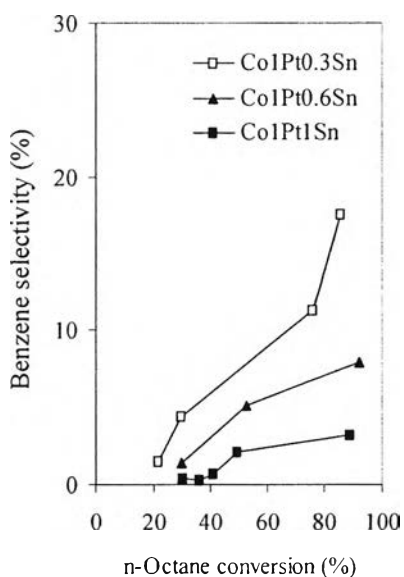
Figure 6.12 The variation of benzene selectivity with n-octane conversion of various Sn/Pt ratios of the bimetallic Pt-Sn/KL catalysts prepared by vapor phase co-impregnation; reaction conditions: temperature = 500°C, pressure = 1 atm, WHSV = 0.5-5 h^{-1}, and H$_2$:HC = 6:1.
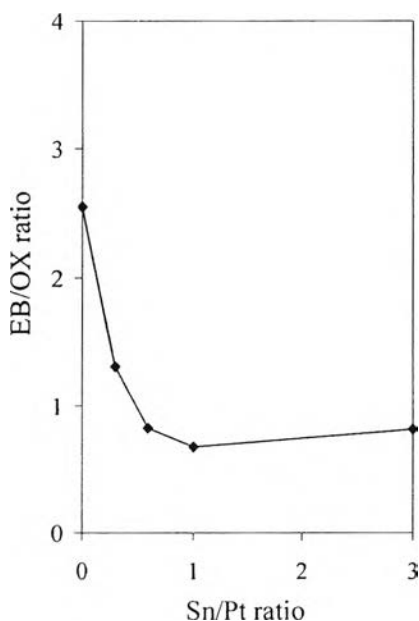

Figure 6.13 The variation of EB/OX ratio with Sn/Pt ratios of the bimetallic Pt-Sn/KL catalysts prepared by vapor phase co-impregnation; reaction conditions: temperature = 500°C, pressure = 1 atm, WHSV = 5 h^{-1}, and H$_2$:HC = 6:1.
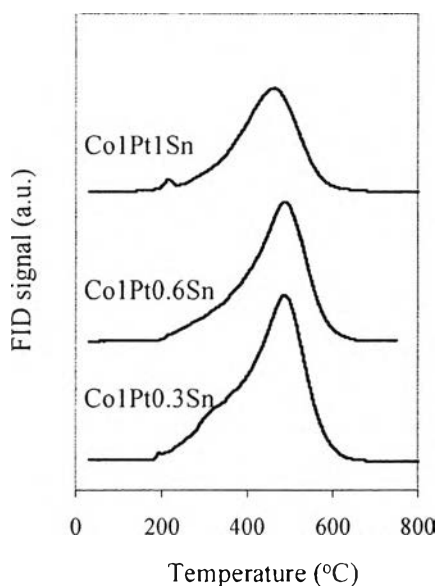
Figure 6.14 TPO profiles of various Sn/Pt ratios of the bimetallic Pt-Sn/KL catalysts prepared by vapor phase co-impregnation method.

6.5 Conclusions

The bimetallic Pt-Sn/KL catalysts exhibited the stability, and selectivity to C8-aromatics compared to the monometallic 1Pt catalyst. The stability of bimetallic Pt-Sn/KL was improved because tin inhibited the adsorption of dehydrogenate species which is the intermediate for formation of coke. Furthermore, it was found that the bimetallic Pt-Sn/KL catalyst prepared by vapor phase co-impregnation (Co1Pt1Sn) exhibited good activity compared to that prepared by sequential method because it gave the high fraction of PtSn alloy phase. The hydrogenolysis reaction which is occurred inside the pore of KL zeolite was inhibited due to the geometric and electronic effects. Moreover, the electrons transfer from tin atoms to Pt atoms causes the high selectivity of C8-aromatic products, especially for OX molecules.

Comparison between the catalytic performance of CO1Pt1Sn and that of Pt-Sn/SiO$_2$ results two important conclusions for aromatization which are:

1. At a low conversion, even the KL zeolite is necessary for using as the support for the aromatization of n-octane since the formation of aromatics is easily generated inside the pore of KL zeolite compared to silica which is a non-

microporous support; however, the hydrogenolysis reaction still have affect on the aromatization of n-octane. Therefore, less C8-aromatics product was produced at low conversion and no difference in the selectivity to C8-aromatics between Co1Pt1Sn and PtSn/SiO$_2$ was observed at low conversion.

2. At a high conversion, Pt-Sn/SiO$_2$ which formed perfect PtSn alloy phase exhibited the high selectivity to C8-aromatics and less selectivity to hydrogenolysis products compared to Co1Pt1Sn. The addition of Sn can improve the catalytic performance for aromatization of n-octane when high fraction of PtSn alloy phase was observed. At this condition, the using of KL zeolite is not necessary since less selectivity to alkenes is observed.

6.6 Acknowledgements

6.7 References

1. Meriaudeau, P. and Naccache, C., Catal. Rev.-Sci. Eng. 39(1&2), 3 (1997).

2. Bernard, J.R,Proceeding in 5th International Conference on Zeolite, L.V.C. Ress (Ed), Heyden, London 686 (1980).

3. Lane, G, Modica, F.S. and Miller, J.T., J. Catal. 129, 145 (1991).

4. Hughes, T.R., Buss, W.C., Tamm, P.W. and Jacobson, R.L., Stud. Surf. Sci. Catal. 28, 725 (1986).

5. Tamm, P.W., Mohr, D.H. and Wilson, C.R., Stud. Surf. Sci. Catal. 38, 335 (1988)

6. Jongpatiwut, S., Sackamduang, P., Osuwan, S., Rirksomboon, T. and Resasco, D.E., J. Catal. 218, 1 (2003).

7. Jongpatiwut, S., Sackamduang, P., Rirksomboon, T. Osuwan, S. Alvarez, W.E. and Resasco, D.E., Appl. Catal. A General 230, 177 (2002.

8. Jacobs, G., Ghadiali, F., Pisano, A., Borgna, A., Alvarez, W.E and Resasco, D.E., Appl. Catal A. General 188, 79 (1999).

9. Jacobs, G., Alvarez, W.E. and Resasco, D.E., Appl. Catal. A. General 206, 267 (2001).

10. Arika, J., Italbashi, S. and. Tamura, Y., US Pat. 4 530 824 (1985).

11. Davis, B.H., Catal. Today 53, 443 (1999).

12. Antos, G.J.,. Aitani, A.M. and Parera, J.M.,Catalytic Naphtha Reforming: Science and Technology 61 (1995).

13. Lietz, G.,. Thoand, H.S and Volter, J., J. React. Kinet. Catal. Lett. 21 429 (1982).

14. Davis, R.J., HCR Concise Review, John Wiley and Sons, New York (1994).

15. Jongpatiwut, S., Trakarnroek, S., Rirksomboon, T., Osuwan, S. and. Resasco, D.E., Catal. Lett. 100, 7 (2005).

16. Verduijn, J.P., Int. Pat. WO 91/06367 (1991).

17. Ertl, G., Knozinger, H. and Weitkamp, J., Handbook of Heterogeneous Catalysis 5, 2143 (1997).

18. Paal, Z., Gyory, A., Uszkurat, I., Olivier, S., Guerin, M. and Kappenstein, C., J.Catal.168, 164 (1997).

19. Macleod, N., Fryer, J.R., Stirling, D. and Webb, G., Cat. Today 46, 37 (1998).

20. Rangel, M.C., Carvalho, L.S., Reyes, P., Parera, J.M. and Figoli, N.S., Catal. Lett. 64, 171 (2000).

21. Passos, F.B.., Aranda, D.A. and Schmal, M., J.Catal. 178, 478 (1998).

22. Lee, S.H. and Lee, H.L., Korean. J. of. Chem. Eng. 1103, 185 (1994).

23. Cho, S.J. and Ryoo, R., Catal. Lett. 97, 71 (2004).

24. Hill, J.M., Cortright, R.D. and Dumesic, J.A., Appl. Catal.A. General 168, 9 (1998).

25. Cortright, R.D., Hill, J.M. and Dumesic, J.A., Catal. Today 55, 213 (2000).

26. Cortright, R.D. and Dumesic, J.A., J. Catal. 148, 771 (1994).

27. Shi, B. and Davis, B.H., J. Cata. 162, 134 (1996).

28. Klepel, O., Breitkopf, C. and Standke. M., J. Mol. Cata. A:Chem. 210 (1&2), 211 (2004).

29. Jacobs, G., Padro, C.L., and Resasco, D.E., J. Catal. 179, 43 (1998).

30. Ostgare, D.J., Kustov, L., Poeppeimeier, K.R., J.Catal. 133(2), 342 (1992).

31. Zheng, J., Dong, J., Xu, Q. and Hu, C., Catal. Lett. 37, 25 (1996).

32. Rodriguez, R., Pfaff, C., Melo, L. and Betancourt, P., Catal. Today 107-108, 100 (2005).

33. Balakrishnan, K. and Schwank, J. , J. Catal. 127, 287 (1991).

34. Volter, J., Lietz, G., Uhlemann, M., and Hermann, M., J. Catal. 68, 42 (1981).

35. Lieske, H., and Volter, J., J. Catal. 90, 96 (1984).

36. Palazov, A., Bonev, C.H., Shoppov, D., Lietz, G., Sarkany, A., and Volter, J., J.Catal. 103, 249 (1987).

37. Kim, K.S., Winograd, N., Davis, R.E., J. Am. Chem. Soc. 93, 6296 (1971).

38. Morales, R., Melo, L., Llanos, A., Zaera, F., J. Mol. Catal. A: Chem. 228, 227 (2005).

39. Li, Y. and Klabunde, K.J., J. Catal. 126, 173 (1990).

40. Llorca, J., Homs, N., Leon, J., Sales, J., Fierro, J.L.G., and Ramirez de la Piscina, P., Appl. Catal. A. General 189, 77 (1999).

41. Hill, J.M., Cortright, R.D. and Dumesic, J.A., Appl. Catal.A. General 168, 9 (1998).

42. Stagg, S.M., Querini, C.A., Alvarez, W.E. and Resasco, D.E., J.Catal. 168, 75 (1997).

43. Westfall, G.A., Pezzanite, J.O. and Davis, B.H., J.Catal. 42, 247 (1976).

44. Lee, S.W. and Lee, H.I., Korean J. Ind.&Eng.Chem. 4, 569 (1993).

45. Davis, B.H. and Venuto, P.B., J. Catal. 15, 363 (1969).